

Electronic Supplementary Information

Waste cotton cloth derived carbon microtube textile: a robust and scalable interlayer for lithium-sulfur batteries

Bangbei Zheng,^{ab} Narui Li,^{ab} Jiaye Yang^{ab} and Jingyu Xi^{*a}

^a Institute of Green Chemistry and Energy, Graduate School at Shenzhen, Tsinghua University, Shenzhen 518055, China. E-mail: xijy@tsinghua.edu.cn

^b School of Materials Science and Engineering, Tsinghua University, Beijing 100084, China

Experimental Section

Preparation of CCC interlayers

The CCC was obtained by the direct carbonization of the cotton cloth.¹ Typically, a large piece of cotton cloth (25 × 10 cm) was folded into five stacks and carbonized at 950 °C for 2 h under Ar gas atmosphere with a heating rate of 5 °C min⁻¹. After cooling down, the CCC was punched into circular interlayers with a diameter of 19 mm. The scalable preparation of the CCC interlayers is beneficial to the consistency of the experimental materials and the reproducibility of the experimental results.

Preparation of sulfur cathode and cell assembly

The sulfur cathode was fabricated using the slurry-coating method.² 60 wt.% sulfur, 30 wt.% Super P and 10 wt.% polyvinylidene fluoride (PVDF) were firstly dried at 60 °C in a vacuum oven for 2.5 h and then dissolved in N-methyl-2-pyrrolidone (NMP). The mixtures were stirred for 5 h to form a homogeneous slurry. Finally the slurry was casted on a carbon coated aluminum foil and dried at 55 °C for 12 h in a vacuum oven. The areal mass loading of sulfur in the cathode was about 1.0 mg cm⁻². The cathode with a higher sulfur loading of 2.0 mg cm⁻² was prepared in the same procedure. CR2025 coin cells were assembled in an Ar-filled glove box. The pure lithium foil was used as the anode. PP separator was used as the separator with a CCC interlayer inserted between it and the sulfur cathode. The electrolyte was 1 M lithium bis(trifluoromethanesulfonyl)imide (LiTFSI) and 1 wt.% LiNO₃ in DOL and DME solution (1:1 by volume). For the Li-S batteries based on PP separator, 40 μL electrolyte was placed on the two sides of the PP separator equally. For the Li-S batteries based on the CCC interlayer, the volume of the electrolyte in the anode side was 20 μL and 60 μL electrolyte was placed on the cathode side to fully wet the CCC interlayer. To ensure the reproducibility of the electrochemical performances of the Li-S batteries, we fabricated the Li-S batteries

that are conducted parallel tests with the same group sulfur cathodes and experimental materials.

Characterization

Morphology of the samples was observed using the scanning electron microscope (SEM, ZEISS SUPRA 55). The transmission electron microscope (TEM, JEOL JEM-3200FS) was employed to acquire TEM image. Raman spectroscopy was gained by the Raman spectrometer (Horiba LabRAM HR800). The X-ray photoelectron spectrometer (XPS, Thermo Fisher ESCALAB 250Xi) was used to obtain the XPS spectrum. Contact angle measurements were conducted on the contact angle measuring instrument (POWEEACH, JC2000D1). The porosity character was analyzed by the accelerated surface area and porosimetry system (ASAP 2020M+C).

Electrochemical measurements

Cyclic voltammetry (CV) measurements were performed on the electrochemical workstation (Chenhua, CHI650b), of which the voltage window was 1.7-2.8 V and the scanning rate was 0.1 mV s^{-1} . Electrochemical impedance spectroscopy (EIS) measurements were carried out on the electrochemical workstation (Bio Logic, VMP3) with a frequency range of 100 kHz to 10 mHz. The cycling performance and the rate capability were tested on the battery testing system (Neware, CT-4008-5V10mA) at room temperature ($25 \pm 2 \text{ }^\circ\text{C}$). The voltage window was also 1.7-2.8 V.

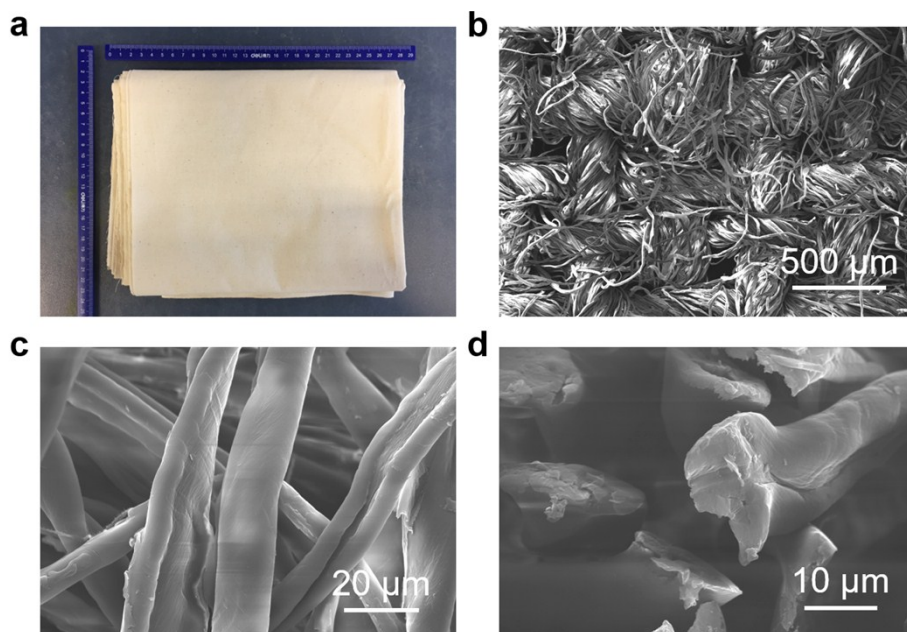


Fig. S1 (a) Photograph, (b-c) SEM images, and (d) cross-sectional SEM image of the cotton cloth.

Fig. S1 shows the photograph, SEM images, and cross-sectional SEM image of the cotton cloth. As displayed clearly, the cotton cloth shows a knitted structure (b). The diameter of single fiber ranges from 10 to 15 μm roughly (c) and the cross-sectional SEM image (d) indicates that the fibers are solid before carbonization.

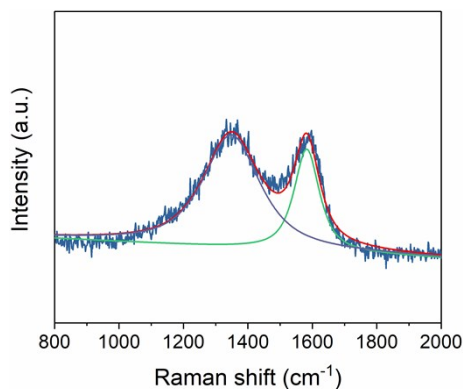


Fig. S2 Detaily fitted Raman spectrum of the CCC interlayer.

Fig. S2 demonstrates the detaily fitted Raman spectrum of the CCC interlayer. It shows two bands around 1349 and 1583 cm^{-1} , respectively. The band at around 1349 cm^{-1} , denoted as D (disordered) mode, is ascribed to the phonons near the Brillouin zone boundary active in small crystallites or on the boundaries of large crystallites. The band at around 1583 cm^{-1} , often called as G (graphitic) mode, is attributed to the “in-plane” zone-center atomic vibrations of large graphite crystallites. There exists no apparent signal of amorphous carbon (A mode).^{3,4} The integrated intensity of the D mode is much larger than that of the G mode, indicating the low graphitic degree of the CCC interlayer.

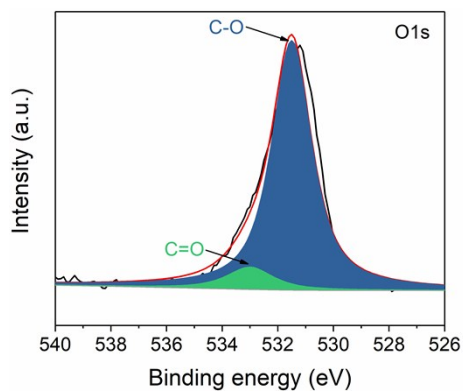


Fig. S3 High resolution O1s XPS spectrum of the CCC interlayer.

The high resolution O1s XPS spectrum of the CCC interlayer is depicted in Fig. S3. It displays two peaks at 531.5 and 533.0 eV, attributed to the C-O and C=O bonds, respectively.⁵ The content of O element in the CCC interlayer is 13.32 at%.

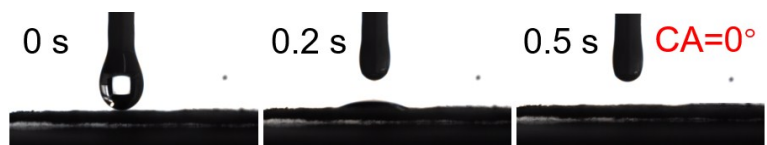


Fig. S4 Electrolyte contact angle of the CCC interlayer.

Fig. S4 demonstrates the electrolyte contact angle of the CCC interlayer. The electrolyte is immediately absorbed in 0.5 s and the contact angle is almost 0° , implying the superior wettability of the CCC interlayer.



Fig. S5 Photograph of the resistance measurement of the CCC by the multimeter.

The electronic conductivity of the CCC interlayer is roughly tested by a simple resistance measurement.

The size of the tested CCC is about $7.2 \text{ cm} \times 3.6 \text{ cm} \times 300 \text{ }\mu\text{m}$. The resistance of the tested CCC is $38.9 \text{ }\Omega$.

It is calculated that the electronic conductivity of the CCC interlayer is about 171.4 S m^{-1} .

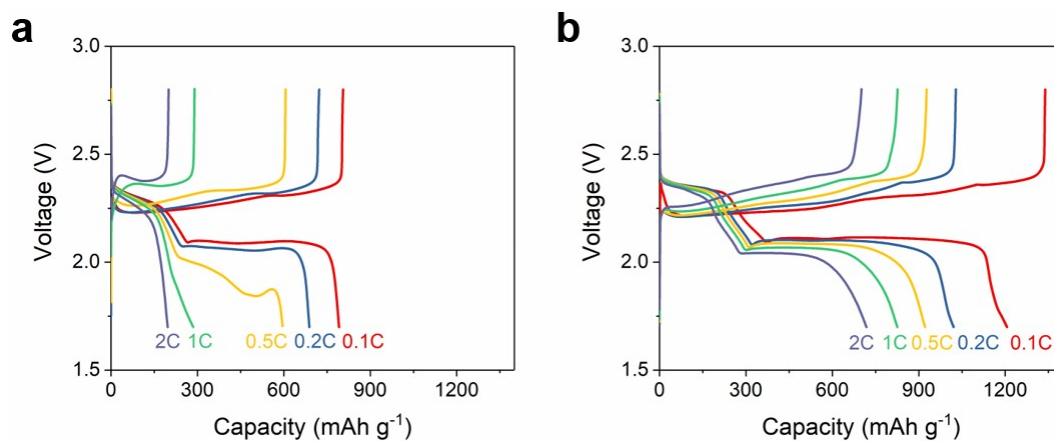


Fig. S6 The charge-discharge curves of the Li-S batteries based on PP separator (a) and the CCC interlayer (b) at different rates.

Fig. S6 exhibits the charge-discharge curves of the Li-S batteries based on PP separator (a) and the CCC interlayer (b) at different rates. Obviously, the two voltage plateaus appear in the discharge curves of the Li-S battery based on PP separator only at low current densities of 0.1 and 0.2 C. When the current density increases to 1 C, the lower voltage plateau nearly disappears, resulting in huge polarization and low specific discharge capacity.⁶ Contrarily, the discharge curve of the Li-S battery based on the CCC interlayer still presents two voltage plateaus even at a large current density of 2 C, leading to smaller polarization and relatively high discharge capacity.

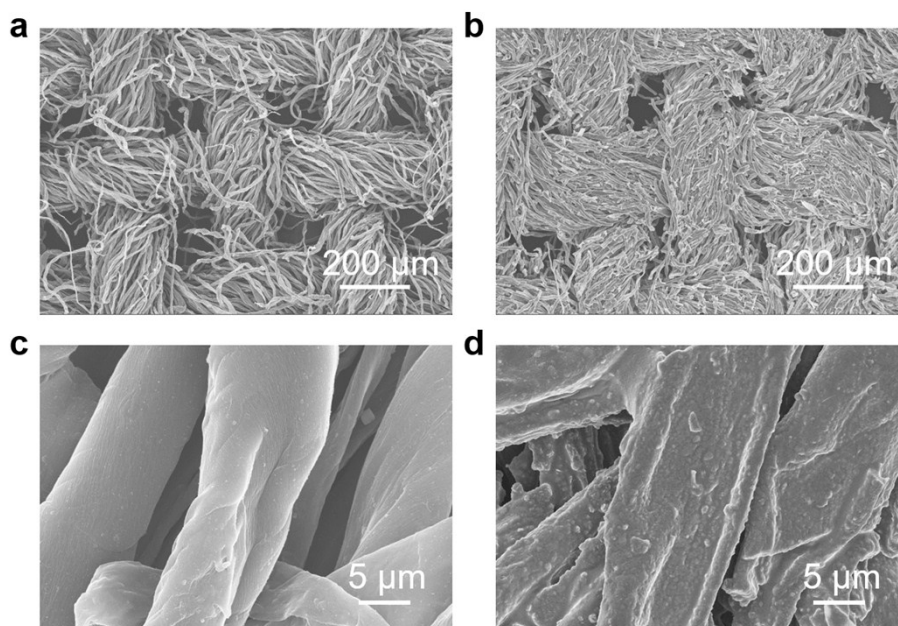


Fig. S7 SEM images of the CCC interlayer before cycling (a, c) and after 500 cycles at 0.5 C (b, d).

Fig. S7 demonstrates the SEM images of the CCC interlayer before cycling and after 500 cycles at 0.5 C. Before cycling, the CCC interlayer shows a knitted structure (a) and the carbon microtubes present smooth surfaces (c). After cycling, the surfaces of the carbon microtubes become coarse (d) owing to the deposition of LIPS and the electrolyte salts.⁷ Importantly, the knitted structure is completely preserved even after 500 cycles (b), implying the structure stability of the CCC interlayer.

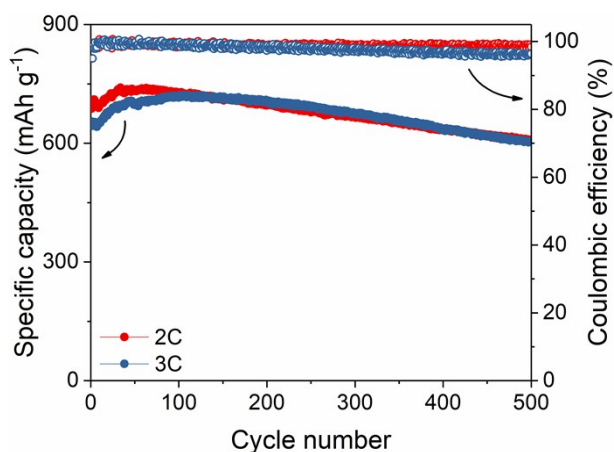


Fig. S8 The cycling performances of the Li-S batteries based on the CCC interlayer at high current densities of 2 and 3 C.

The cycling performances of the Li-S batteries based on the CCC interlayer at high current densities of 2 and 3 C are displayed in Fig. S8. They deliver initial discharge capacities of 688 and 655 mAh g⁻¹ at 2 and 3 C, respectively. Correspondingly, high discharge capacities of 607 and 605 mAh g⁻¹ after 500 cycles are reserved. The capacity decay rates are as low as 0.024% and 0.015% per cycle, showing the good cycling performances of the Li-S batteries based on the CCC interlayer at large current densities.

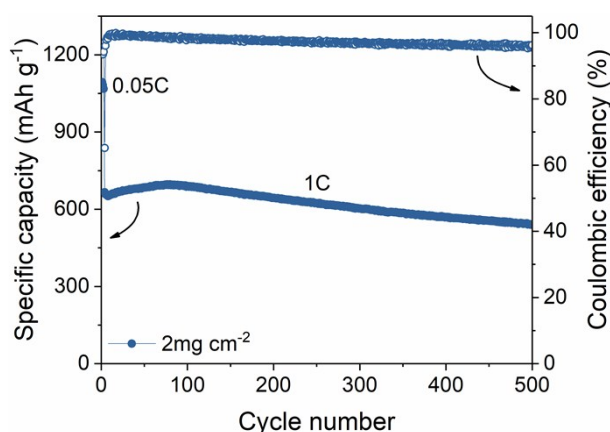


Fig. S9 The cycling performance of the Li-S battery based on the CCC interlayer with higher sulfur loading of 2 mg cm^{-2} at 1 C.

Fig. S9 exhibits the cycling performance of the Li-S battery based on the CCC interlayer with higher sulfur loading of 2 mg cm^{-2} at 1 C. The Li-S battery displays an initial discharge capacity of 1094 mAh g^{-1} at 0.05 C. After three cycles of activation, it delivers 666 mAh g^{-1} at 1 C and holds 541 mAh g^{-1} after 500 cycles.

References

- 1 M. Cakici, R. R. Kakarla and F. Alonso-Marroquin, *Chem. Eng. J.*, 2017, **309**, 151-158.
- 2 B. Zheng, L. Yu, Y. Zhao and J. Xi, *Electrochim. Acta*, 2019, **295**, 910-917.
- 3 S. Liu, J. Li, X. Yan, Q. Su, Y. Lu, J. Qiu, Z. Wang, X. Lin, J. Huang, R. Liu, B. Zheng, L. Chen, R. Fu and D. Wu, *Adv. Mater.*, 2018, **30**, 1706895.
- 4 Y. Tang, S. Liu, B. Zheng, R. Liu, R. Fu, D. Wu, M. Zhang and M. Rong, *Chem. Commun.*, 2018, **54**, 11431-11434.
- 5 X. Qin, J. Wu, Z.-L. Xu, W. G. Chong, J.-Q. Huang, G. Liang, B. Li, F. Kang and J.-K. Kim, *Carbon*, 2019, **141**, 16-24.
- 6 L. Luo, X. Qin, J. Wu, G. Liang, Q. Li, M. Liu, F. Kang, G. Chen and B. Li, *J. Mater. Chem. A*, 2018, **6**, 8612-8619.
- 7 K. Yang, L. Zhong, Y. Mo, R. Wen, M. Xiao, D. Han, S. Wang and Y. Meng, *ACS Appl. Energy Mater.*, 2018, **1**, 2555-2564.